AD NUMBER

**ADB017344**

LIMITATION CHANGES

TO:

**Approved for public release; distribution is unlimited.**

FROM:

**Distribution authorized to U.S. Gov't. agencies only; Test and Evaluation; JAN 1977. Other requests shall be referred to Air Force Armament Laboratory, Attn: DLYV, Eglin AFB, FL 32542.**

AUTHORITY

**USADTC ltr, 23 Oct 1979**

# AFATL-TR-77-1, VOLUME I

# INVESTIGATION OF OBLIQUE SHOCKS AND EDGE EFFECTS FOR UNDERGROUND TARGETS VOLUME I. OBLIQUE SHOCKS

ORLANDO TECHNOLOGY, INCORPORATED
6237 EDGEWATER DRIVE
ORANDO, FLORIDA 32810



JANUARY 1977

FINAL REPORT: DECEMBER 1975 - JUNE 1976



AIR FORCE ARMAMENT LABORATORY
AIR FORCE SYSTEMS COMMAND • UNITED STATES AIR FORCE
EGLIN AIR FORCE BASE, FLORIDA

SECURITY CLASSIFICATION OF THIS PAGE (When Data Entered)

# REPORT DOCUMENTATION PAGE

READ INSTRUCTIONS BEFORE COMPLETING FORM

1. REPORT NUMBER: AFATL-TR-77-1, Volume I

2. GOVT ACCESSION NO:

3. RECIPIENT'S CATALOG NUMBER:

4. TITLE (and Subtitle): INVESTIGATION OF OBLIQUE SHOCKS AND EDGE EFFECTS FOR UNDERGROUND TARGETS. VOLUME I: OBLIQUE SHOCKS.

5. TYPE OF REPORT & PERIOD COVERED: Final Report: December 1975 - June 1976

6. PERFORMING ORG. REPORT NUMBER:

7. AUTHOR(s): Hans R. Fuehrer; John W. Keeser

8. CONTRACT OR GRANT NUMBER(s): F08635-76-C-0155 NEW

9. PERFORMING ORGANIZATION NAME AND ADDRESS:
Orlando Technology, Incorporated
6237 Edgewater Drive
Orlando, Florida 32810

10. PROGRAM ELEMENT, PROJECT, TASK AREA & WORK UNIT NUMBERS:
Project No. 9134
Task No. [illegible] 06
Work Unit No. 004

11. CONTROLLING OFFICE NAME AND ADDRESS:
Air Force Armament Laboratory
Armament Development and Test Center
Eglin Air Force Base, Florida 32542

12. REPORT DATE: Jan[illegible] 1977

13. NUMBER OF PAGES: 52

14. MONITORING AGENCY NAME & ADDRESS (if different from Controlling Office): 52p.

15. SECURITY CLASS. (of this report): Unclassified

15a. DECLASSIFICATION DOWNGRADING SCHEDULE:

16. DISTRIBUTION STATEMENT (of this Report)
Distribution limited to U. S. Government agencies only; this report documents test and evaluation; distribution limitation applied January 1977. Other requests for this document must be referred to the Air Force Armament Laboratory (DLYV), Eglin Air Force Base, Florida 32542.

17. DISTRIBUTION STATEMENT (of the abstract entered in Block 20, if different from Report): AFATL TR-77-1-Vol-1

18. SUPPLEMENTARY NOTES

Available in DDC

19. KEY WORDS (Continue on reverse side if necessary and identify by block number)

Underground Targets
Oblique Shocks and Edge Effects
Earth Shock
Structure Survivability
Analytical Target Vulnerability Analysis
Free Surface Tests
Constrained Configuration Tests
Displacement Time Data
Earth/Concrete Interface Interaction

20. ABSTRACT (Continue on reverse side if necessary and identify by block number)

This report summarizes results of a six-month test and analysis program to establish the effects of oblique shock waves on buried concrete structures. The objective of this program was to generate basic test data which would show the effects of various corner angles (20 to 160 degrees) on a shock wave impinging a buried structure. The transmitted impulse was measured by photographic and electronic means. The initial velocity of a steel fly-off

DD FORM 1 JAN 73 1473 EDITION OF 1 NOV 65 IS OBSOLETE

UNCLASSIFIED
SECURITY CLASSIFICATION OF THIS PAGE (When Data Entered)

391064

plate was obtained from high-speed photography. Quartz pressure gages were used to measure maximum force and total impulse as a function of the corner angle. Maximum force was found to be relatively constant at 20-, 30-, and 45-degree corner angles, drop sharply at 60 degrees and climb steadily from 90- to 160-degree corner angles. Initial fly-off velocity followed a similar pattern decreasing at 60 degrees, then rising steadily. The force reduction at 60 degrees may be the result of the formation of a Mach stem along the cone surface. Recommendations are to use hydrodynamic computer codes to better identify the mechanism involved, and to continue experimentation using the quartz pressure gages and vary charge weight, stand-off, and other parameters to fully resolve effects of shock coupling with oblique geometries.

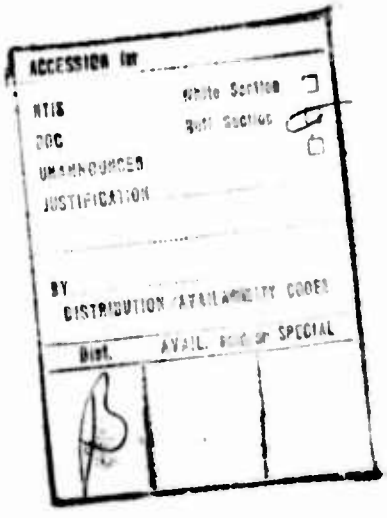

# SUMMARY

This section summarizes the overall objectives of a program conducted toward providing data to establish breach criteria for underground structures. Program objectives are presented, followed by a summary of findings and recommendations.

## A. PROGRAM OBJECTIVES

Hard targets, composed of concrete structures placed underground or covered with soil, may be defeated by one of two means: (1) small kinetic energy penetrating weapons detonating inside the structure, and (2) the propagation of earth shock from a large high explosive weapon detonating externally near the structure. The ultimate goal of defeating the hard target is the destruction of the contents which may consist of personnel, ammunition, supplies, electronic equipment, or fuel. It is evident that destruction of the hard target will result in destruction of the contents. It would also prevent its further use as a protective structure. This level of damage may be accomplished only by the placement of an explosive charge sufficiently close to the structure to cause its structural integrity to be lost. This loss of structural integrity can be accomplished through breach of the structural walls as a result of the earth/concrete interface interaction. Thus, the propagation of earth shock and its interface with concrete structure becomes of primary concern.

Analytical target vulnerability analysis cannot be expected to produce realistic and usable data unless it is based on sound experimental test results and makes use of reliable damage prediction techniques. It therefore becomes necessary to conduct basic experimental test programs to generate empirical data which will provide a baseline for conducting analytical studies. The primary damage mechanism to be investigated in this effort is earth shock. The primary target of interest is buried concrete structures. The objectives of this program are (1) to obtain experimental data concerning the effects of oblique shocks impinging on buried structures and, (2) to determine basic information on survivability of a structure which has increased stiffness and strength around its edges and corners.

## B. PROGRAM FINDINGS

In order to investigate oblique shock and its effects for

underground tests, a two-phase program was established. The first phase was entitled "Oblique Shocks," and the results are reported in this volume. The second phase, "Edge Effects," is reported in Volume II.

1. Oblique Shocks

As an explosive charge detonates in soil, the shock wave radiates from the explosive charge outward, and when it impinges upon a concrete structure the angle can vary from normal incidence (face-on pressure) to a 90-degree incidence (side-on pressure) configuration. Under static conditions it is expected that the side-on pressure normally is about one-third of the hydrostatic pressure being generated at that level. However, with shock front, one must not only consider the hydrostatic overpressure behind the shock but particle velocities in the form of the dynamic pressure. A test configuration was chosen that is axisymmetrical using the cylindrical geometry configuration. This geometry is amenable to theoretical analysis using available continuum mechanics codes.

For this series of tests, a concrete cone with a cylindrical top was constructed. The total angle of the cone portion was varied from 20 to 160 degrees, while the height of the cylindrical portion was varied to keep the total weight constant. This geometry enables one to investigate the relationship between cone angle and coupling efficiency of the explosive energy.

The initial tests were a series to measure the impulse imparted to the structure by the charge as determined from its initial velocity. The test configuration is a variation on the ballistic pendulum type of test where an object is given an initial impulse and its height is determined to establish its initial velocity, and thus the impulse. In these tests high-speed photography was used to track the vertical trajectory of the test structure so that its initial velocity was obtained. By plotting the initial velocity as a function of cone angle, an indication of the impulse absorbed by the test structure as a function of cone angle was obtained.

A second series of tests used the same basic configurations but constrained the top surface and measured the force as a function of time. Computing the area under the force-time curve, the impulse was determined. The force and impulse as a function of the cone angle were then determined.

Thirty-six tests were conducted to measure the free surface velocity of the concrete-steel mass, and seven tests were

conducted to measure the force when the steel plate is constrained from free motion. These tests showed that use of hydrostatic-type loading and simple geometrical considerations do not adequately predict the actual response. At shallow angles, force levels above those predicted by an inverse square or inverse cube relationship exist. Further, a definitive anomaly occurs in the impulse data when tests were conducted using 60- and 135-degree cones.

2. Edge Effects

The angle at which a shock wave encounters a concrete structure can vary from face-on to side-on, the latter being 90-degree incidence. At a corner, one finds the geometry such that, in general, neither extreme is reached. Rather, a continually varying geometry exists. Thus, armed with oblique shock data generated during the first phase of this program, tests were conducted on cubical reinforced concrete structures. Reinforcement was at the two-percent level with wall thickness of 4 and 8 inches. If these are viewed as one-third scale structures, they simulate two-percent reinforced concrete structures with 1- and 2-foot-thick walls. Conversely, the 4-inch wall structure is a one-half scale model of the 8-inch-thick structure.

Charges of the high explosive C-4 were buried at various positions to provide breach data as a function of charge weight and position. Also, measurements of free-soil pressure were made. By plotting the data, a breach contour was suggested and documented with supporting data.

Based on the charge orientation tests, near-field effects are quite evident. Pressures off the end of cylindrical charges are much less than those off the side. Thus, charge orientation must be considered.

As part of the underground structure tests, measurements were made of the pressure levels generated in the free soil. This was done to establish whether pressure levels were being generated consistent with that expected from the C-4 charges. The data showed that pressure decreased as the inverse 2.4 power of scaled distance. This value was in contrast to the inverse cube scaling usually employed. However, with the scatter in the data, the inverse cube was also a realistic relationship for the data although not the best least-squares fit.

Eight of the 23 tests made with the underground reinforced concrete structures resulted in breaching. Two conclusions drawn from the data are:

(1) The minimum charge weight that will do breaching damage

must be substantially increased from that predicted from either mid-span breach data or conventional demolition data when used against a corner. Charge weight of 67.5 times the wall thickness in feet cubed should be considered the minimum charge weight for corner breaching.

(2) If a charge weight exceeds minimums required for breaching in contact, the stand-off distance for breach can be computed using methods presented in Volume II.

## C. RECOMMENDATIONS

With reference to the first area of investigation, oblique shocks, it is recommended that a two-phase program be established to further define the soil concrete interface mechanics. The theoretical phase should employ continuum mechanics computer codes to establish shock front phenomena during soil-concrete interface interactions. This work should be coupled with an experimental program designed to continue testing using the constrained test configuration. The results of such a program would further assist in defining underground concrete structure response to earth shock.

Based on the results of the second area of study, edge effects, it is recommended that continued testing be done to better define the effects of several parameters. These are:

(1) Structure thickness-to-span ratio effects in relationship to charge position

(2) Charge orientation

(3) Charge casing

(4) Charge depth

While qualitative effects are known, the need to better define the factors in a quantitative manner exists.

## PREFACE

This report summarizes analytical and experimental investigations conducted from December 1975 through June 1976 by Orlando Technology, Inc., 6237 Edgewater Drive, Orlando, Florida 32810 under Contract F08635-76-C-0155, Investigation of Oblique Shock and Edge Effects for Underground Targets, with the Air Force Armament Laboratory, Armament Development and Test Center, Eglin Air Force Base, Florida. Mr. G. Rickey Griner (DLYV) managed the program for the Armament Laboratory.

This report consists of two volumes. Volume I contains results of experimentation to establish the effects of oblique shock waves on buried concrete structures, and Volume II presents experimental results of tests to determine breach distances in the corner region of buried concrete cubicles. This is Volume I.

Orlando Technology, Inc. Program Manager was Dr. Hans R. Fuehrer. Mr. John W. Keeser, Jr. was a principal contributor.

This technical report has been reviewed and is approved for publication.

FOR THE COMMANDER:

J. R. MURRAY
Chief, Weapon Systems Analysis Division



(The reverse of this page is blank)

TABLE OF CONTENTS


| Section | Title | Page |
|---|---|---|
| I | INTRODUCTION | 1 |
| | A. Background | 1 |
| | B. Objectives | 3 |
| | C. Report Organization | 3 |
| II | FREE-SURFACE TESTS | 4 |
| | A. Test Arrangement | 4 |
| | 1. Photographic Coverage | 4 |
| | 2. Firing Circuit | 7 |
| | 3. Test Assembly | 9 |
| | B. Test Results | 9 |
| | C. Analysis | 11 |
| | D. Conclusions | 17 |
| III | CONSTRAINED CONFIGURATION TESTS | 18 |
| | A. Test Geometry and Set-Up | 18 |
| | 1. Instrumentation | 20 |
| | B. Free-Soil Data | 22 |
| | C. Test Results | 25 |
| | D. Conclusions | 29 |
| IV | CONCLUSIONS AND RECOMMENDATIONS | 30 |
| | A. Conclusions | 30 |
| | B. Recommendations | 31 |
| APPENDICES | | |
| A - | TIME DESPLACEMENT DATA | 32 |
| B - | INVERSE SQUARE AND INVERSE CUBE FUNCTIONS | 39 |
| | REFERENCES | 42 |

LIST OF FIGURES


| Figure | Title | Page |
|---|---|---|
| 1. | Concrete Cone Assembly | 5 |
| 2. | Free-Surface Test Set-Up | 6 |
| 3. | Explosive Fire Control Circuit | 8 |
| 4. | Fire Control System | 7 |
| 5. | Free Surface Test Geometry | 10 |
| 6. | Initial Velocity vs Cone Angle | 16 |
| 7. | Constrained Configuration Test Set-Up | 19 |
| 8. | Electronics System - Constrained Tests | 21 |
| 9. | Kistler Gage and Amplifier | 20 |
| 10. | Free Soil Calibration Test Set-Up | 23 |
| 11. | Free Soil Force Profiles | 24 |
| 12. | Maximum Force Versus Cone Angle | 26 |
| 13. | Total Impulse Versus Cone Angle | 27 |
| B-1 | Forcing Function Versus Cone Angle | 41 |

LIST OF TABLES


| Table | Title | Page |
|---|---|---|
| 1. | Test Summary | 12 |
| 2. | Initial Velocity Data | 15 |
| 3. | Weight of Cone Assembly | 20 |
| 4. | Free Soil Calibration Tests | 25 |
| 5. | Force and Impulse as Function of Cone Angle | 28 |
| A-1 | Displacement-Time Data | 34 |




(The reverse of this page is blank.)

# SECTION I

# INTRODUCTION

This introductory section presents background information pertinent to the entire program reported in Volumes I and II, followed by objectives of work reported in this volume and the organization of the remaining sections.

## A. BACKGROUND

Before 1939, essentially the only systematic investigations of the effects of underground explosions had been the study of remote effects of quarry blasts which had been undertaken by some explosive manufacturers and the U. S. Bureau of Mines in order to establish the limits of distances for certain varieties of superficial damage to dwellings. In 1940, the problem of underground damage became of immediate and pressing interest to the British who initiated a program of experiments to determine crater radii, earth movements, acceleration, and damage radii for bombs. These programs were ad hoc experiments designed to furnish answers to specific pressing problems as they arose and did not attempt a systematic study of the phenomena. Considerable data was accumulated to establish the dimensions of craters and the magnitude of earth movement, both transient and permanent, for various arbitrary depths of explosive charges. A series of full-scale controlled experiments were carried out to assess damage inflicted to underground piping and of model-scale experiments to assess damage to buildings (Reference 1).

More recently, comparisons of results of full-scale and model-scale explosive tests of reinforced concrete protective structures have shown that viable results can be obtained from model tests as small as 1/10 scale (Reference 2). However, the results of the above tests have also indicated that care must be exercised in the preparation of the models and the test site, as well as the performance on the tests, in order to achieve the test data desired (References 3, 4, and 5). Thus, scaling techniques developed in the 1940's and verified repeatedly to the present have shown that it is possible to scale structures and predict behavior of full-scale structures based on the response of model-scale structures. The main advantage of this type of scale-model testing has been to reduce the overall cost within the test program and yet generate viable data. One disadvantage of this testing program is the lack of data which is available to generalize these test results to other configurations.

To provide a better understanding of the physical mechanisms involved, computer programs have been developed which are directed toward prediction of shock strength and ground motion resulting from chemical or nuclear explosions contained in or on the surface of geologic materials. Two-dimensional time-dependent continuum mechanics computer codes have been developed that can be applied to high pressure regions near the explosive source where violent disruption develops, as well as for lower pressure regions where material strength is important. Equations of state have been used to take into account the irreversible compaction of porous materials and also the contribution of internal friction to shear strength. Correlation of nuclear and high explosive sources of the same yield is difficult because of the loss of the large portion of energy of the nuclear source in vaporization of the earth. It has been suggested that an application of an efficiency factor in some form to the nuclear source data serves to provide correlation with the high explosive data and results in a more reasonable correlation (Reference 6). This technique appears viable for those cases where the analysis is done in the lo' er pressure regions where material strength is important. However, in the high pressure region near the explosive source, detailed knowledge of the equations of state of the materials involved is necessary and nuclear vaporization effects cannot be ignored. Hence, efforts are underway to study the soil/concrete interface interactions and concrete structure response to ascertain data for soil behavior in this type of interactive mode.

It is well known from air shock wave propagation work that a mach stem is formed under certain conditions. This formation results in a sustained, higher pressure level being generated. This is due to nonlinear behavior of air at elevated pressures. The initial tests conducted in this work were to establish if, in the case of earth shock impinging on a concrete structure, the phenomenon of sustained and higher pressures could be observed. If this is observed, then one may expect higher damage levels when oblique earth shock impinges on concrete structures.

When one section of a reinforced concrete wall is stiffened by virtue of added thickness or additional reinforcement, then weapon damage mechanism levels generally must be increased. At a corner, both thickness and reinforcement are increased, while the earth shock wave impinges at angles other than normal. This geometry could result in reduced structural loading at points where added strength exists. The second phase of this study deals with the response of structures when earth shock loading occurs at the corners of structures.

Extensive reports have been prepared in the principal practice for design of hardened structures (References 7 and 8) which discuss various methods of analyzing responses of structural elements. When a criterion such as breach is developed in the criteria for structural failure, the response of the structural behavior which is associated with either partial or total failure of the element is characterized by two types of concrete fragmentation: (1) spalling (either direct spalling or scabbing), which is the dynamic disengagement of the surface of the element, and (2) post-failure fragmentation which is associated with structural collapse.

Scabbing of reinforced concrete elements is the end result of a tension failure in the concrete normal to this free surface and is usually associated with large deflections. In the latter stages of the brittle response mode of a reinforced concrete element, extremely large deflections are developed, producing large strains in the structural reinforcement and, consequently, severe cracking and/or crushing of the concrete perpendicular to the free surfaces. Because tension and compression strains are highest at the surface, and since lacing confines the concrete between layers of structural reinforcement at large deflection levels, damage to the concrete is more severe exterior to the reinforcement than between the layers.

## B. OBJECTIVE

The objective of work reported in this volume was to generate experimental data defining the effects of shocks impinging on buried concrete structures with an oblique geometry.

## C. REPORT ORGANIZATION

This volume discusses free surface tests and constraint configuration tests using a concrete cone and steel plate configuration to determine the effect of oblique shock on a concrete/soil interface. Section II of this volume discusses the free surface test. The test arrangement is discussed in the first subsection defining arrangements and instrumentation used. The second subsection briefly discusses the test results, with the third subsection giving the details of the analysis. The fourth subsection presents the conclusions derived from 36 tests conducted within this series. Section III discusses the constraint configuration tests. Section IV summarizes the conclusions and recommendations.

## SECTION II

## FREE-SURFACE TESTS

The purpose of the tests presented in this section was to investigate the energy transfer between an earth shock and a rigid concrete structure. The weight of the structure was held constant and its initial velocity computed from film data, so the effect of earth shock impingment at a relatively constant obliquity angle could be established.

This section discusses the test arrangement, test results, data analysis, and conclusions drawn from 36 experiments.

### A. TEST ARRANGEMENT

In order to study the effects of various corner configurations on shock waves, a set of flat-topped concrete cones was constructed. The cone portion was used to simulate the corner on a buried hardened structure. The cylindrical portion had two purposes: (1) by variations in the height of the cylinder, the weight of the different cones was kept constant, and (2) the flat top of the cylinder was used to impart impulse to the steel fly-off disks placed thereon. Figure 1 is the fabrication drawing for the concrete cones. A lifting sling was attached through the cross pipe to facilitate placement of the cone over the explosive charge.

#### 1. Photographic Coverage

Figure 2 shows a side view of the high-speed camera coverage used during the tests. A camera view of the test geometry is also shown.

The gridded background was used to obtain an accurate displacement-time history of the steel fly-off disk. A high-speed full frame 16mm camera capable of framing rates up to 11,000 pictures per second was used with a timing mark generator, which put marks at 1000 pulses/second on the film edges. These marks allowed exact framing rates to be readily determined.

The camera was fitted with a 75mm lens and loaded with either 4X negative film (Kodak 7224) or Kodak 2470 RAR negative film. These high-speed black and white films were processed

| Cone Angle (degrees) | L (cm) | ℓ (cm) |
|---|---|---|
| 20 | 86.4 | 10.0 |
| 30 | 56.9 | 19.8 |
| 45 | 36.8 | 26.5 |
| 60 | 26.4 | 30.3 |
| 90 | 15.2 | 33.7 |
| 135 | 6.3 | 36.7 |
| 160 | 2.7 | 37.9 |

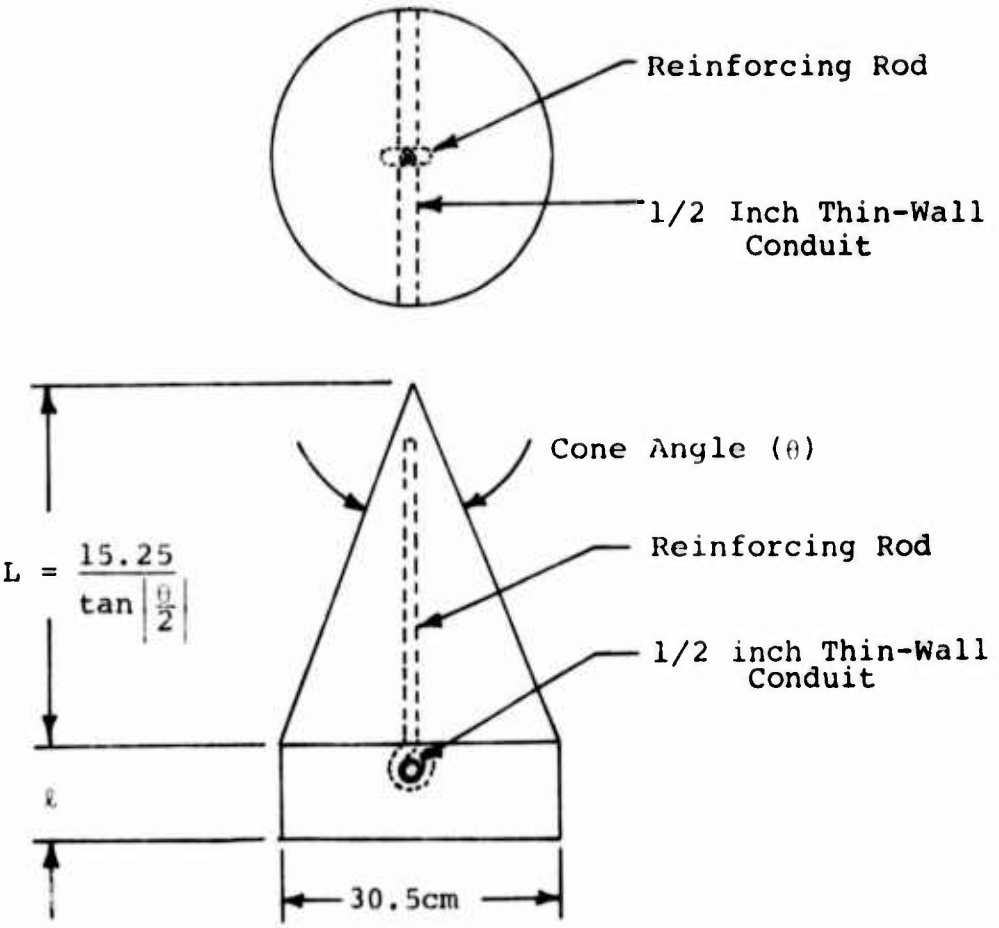


Figure 1. Concrete Cone Assembly

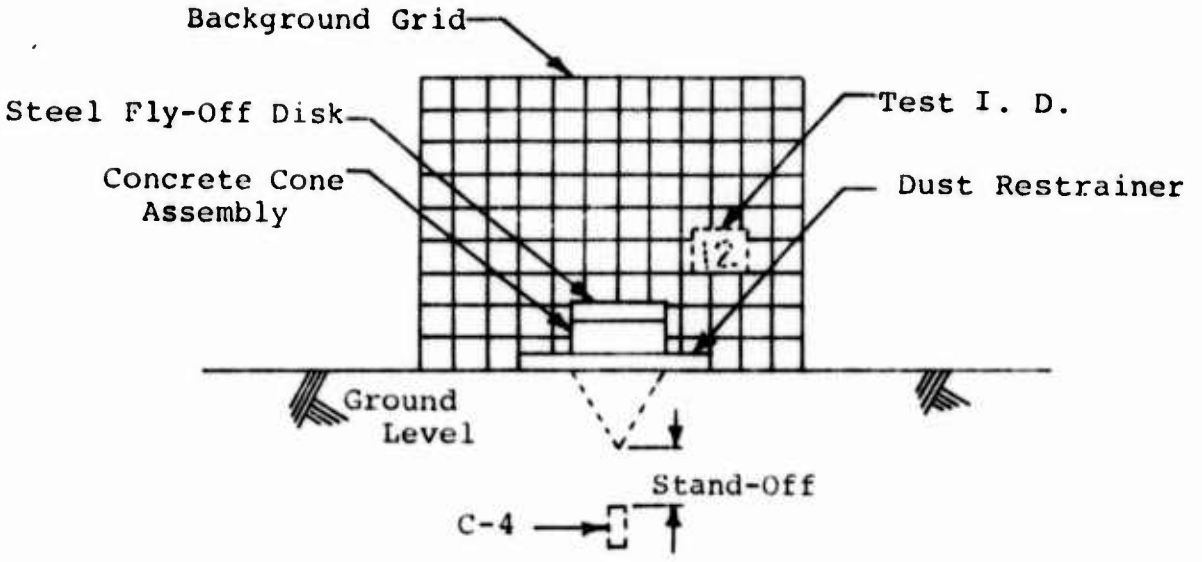


Camera View

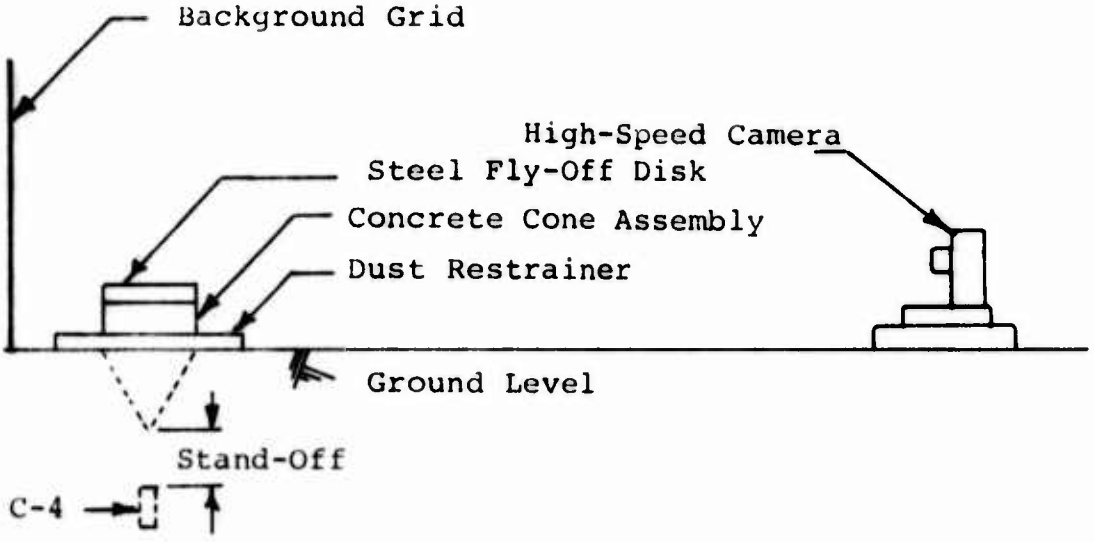


Figure 2. Free-Surface Test Set-Up

to a negative because it was easier to see through dust obscuration in this mode. Filming speed on this camera was varied from 5000 to 10,000 pps, with the aforementioned 1000 pulse/second timing marks applied to the film edge for accurate framing analysis.

The high-speed camera, through use of an adjustable arm riding on the film supply reel, was used to initiate the firing sequence. This technique insured that the cameras had attained sufficient framing speed prior to detonation. The film in each camera thus recorded motion of the steel disks against a gridded background for reduction and analysis.

2. Firing Circuit

The composition C-4 charge was electrically initiated by an automatic control circuit. Figure 3 is a schematic of the complete firing circuit while Figure 4 is a photograph of the control boxes.

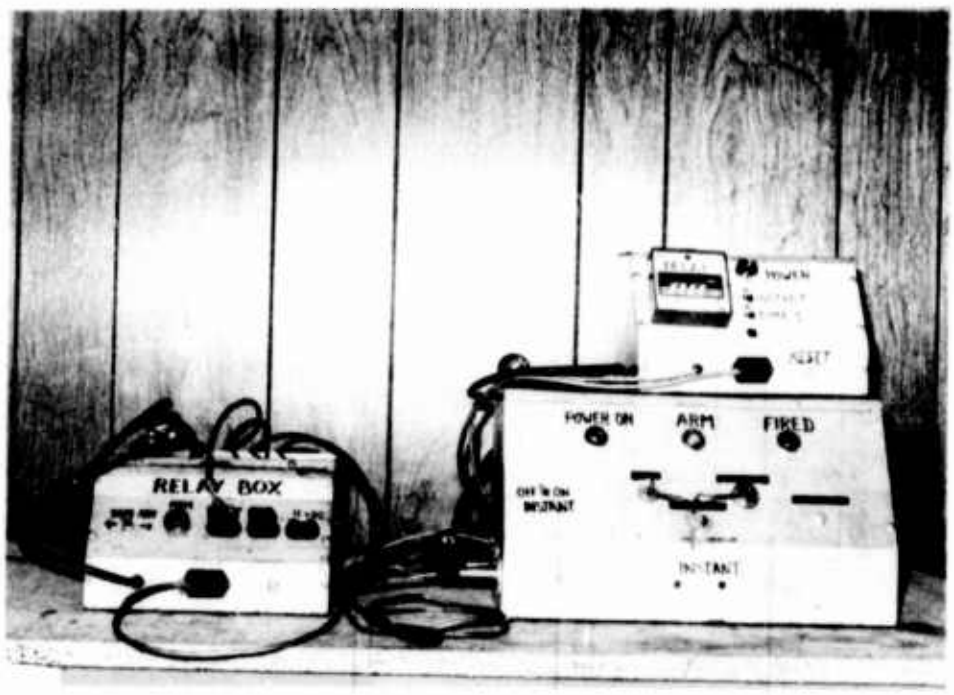


Figure 4. Fire Control System

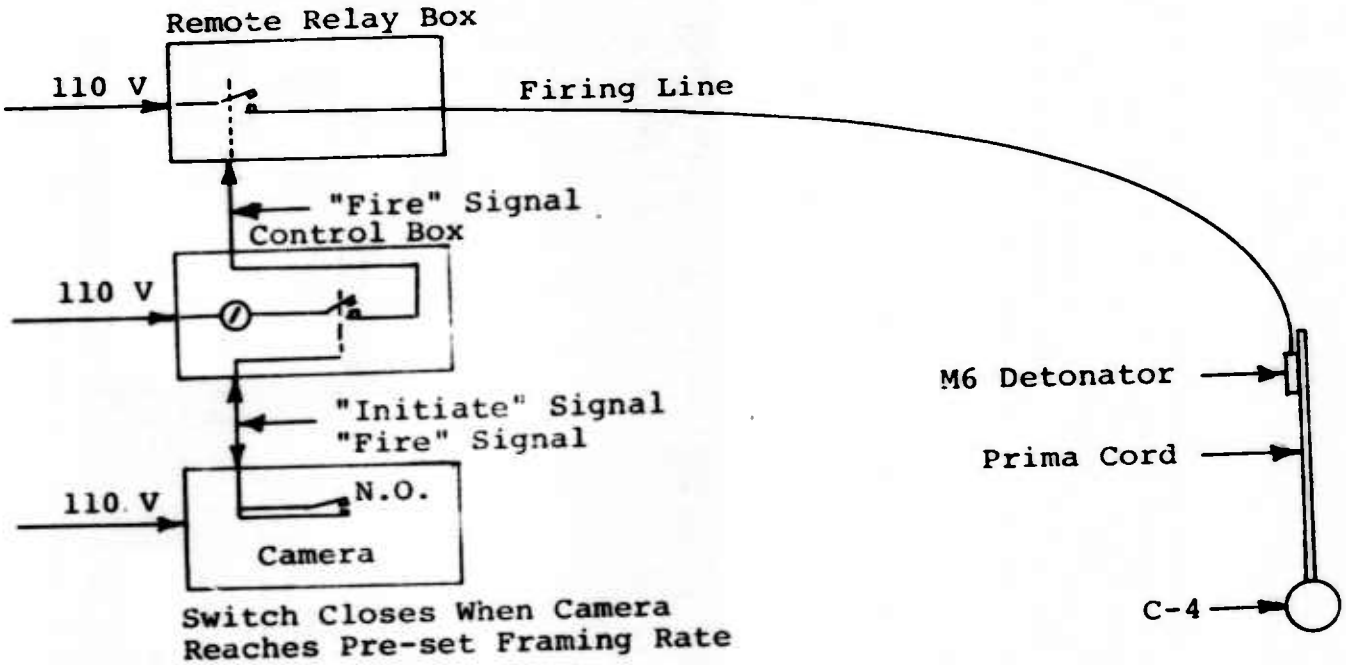


Figure 3. Explosive Fire Control Circuit

The sequence of operations was selected to allow the high-speed camera to control the instant the detonator receives power. This system proved to be easy to operate. By allowing the camera to control the detonator relay, the problem of timing within the system is solved.

3. Test Assembly

A series of tests was run to determine the effects of stand-off distances (15, 30, and 60 cm), cone angle (20, 30, 45, 60, 90, 135, and 160 degrees), and charge size on transmitted impulse. Figure 5 is a cross-section view of a typical test set-up. Note that the test geometry is axisymmetric and therefore compatible with continuum mechanics computer analysis. The explosive charge, because of its small physical size, was formed into a sphere instead of a cylinder. The charge was placed along the extended longitudinal axis of the concrete cone at the specified stand-off. The concrete cone was then positioned and the soil firmly backfilled to bury the explosive charge and the cone to a depth equal to the juncture of the conical section and cylinder.

A steel disk 2 inches thick and 12 inches in diameter was then placed on the horizontal top of the cylinder. The detonating cord, one end of which had been previously affixed to the explosive charge, was dressed off to one side of the test set-up. An additional 2-inch-thick steel annulus (12-inch ID, 24-inch OD) was then lowered over the above-ground portion of the cone/disk assembly. The function of this disk was to constrain surface dust which would otherwise obscure the initial disk motion. The soil surrounding the test set-up was also sprinkled with water immediately prior to each test to further reduce dust.

The explosive train was initiated by an M6 electric cap which was taped to the above-ground end of the detonating cord. This method of explosive initiation insured that, in the case of a misfire, a live detonator would not be imbedded within a buried explosive charge.

The results of these tests are presented in the following subsection.

B. TEST RESULTS

Using the test arrangement described in the previous

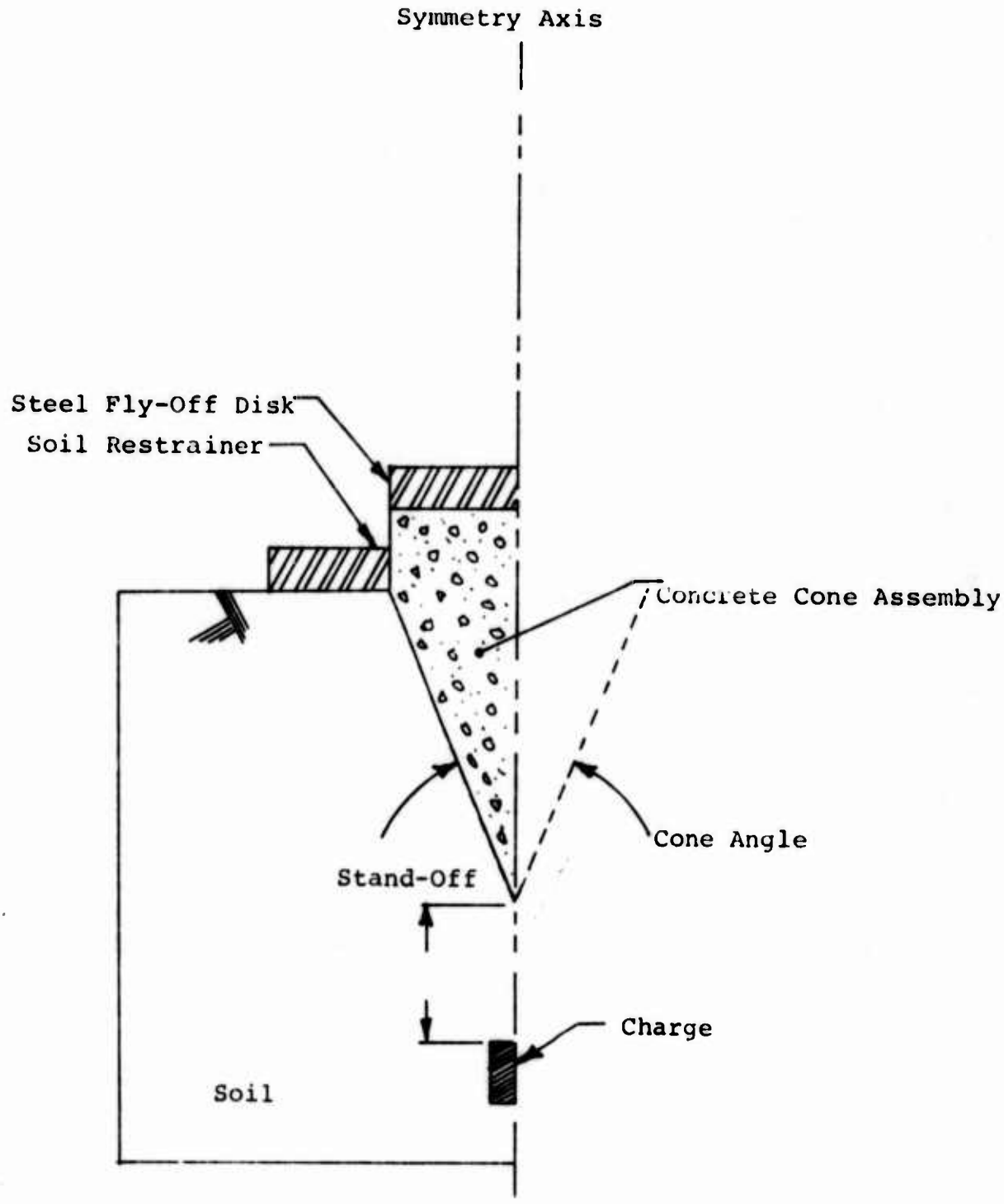


Figure 5. Free Surface Test Geometry

subsection, a total of 36 experiments were conducted. Charge weights of 67.5, 125, 250, and 500 grams were used at positions of contact 15-, 30-, and 60-centimeter stand-offs with the 20-, 30-, 45-, 60-, 90-, 135-, and 160-degree cone angles. Table 1 summarizes the tests giving charge weights, stand-off distances, and cone angle combinations used in each experiment. Initial velocity of the steel flyer plate is included for each test and represents the most salient results.

The upper edge of the steel plate was photographically followed in its upward trajectory. The time it encountered the various displacement heights was noted. Five-centimeter increments were used in the time displacement using the film timing marks and background grid to establish the displacement-time history. Appendix A gives the data of the displacement and time for each of the 36 tests.

The Eglin Air Force Base CDC 6600 computer was used to establish an initial velocity for the plates. A least-squares fit was used to determine the initial velocity as discussed in the following section. However, at this point, it should be noted that the second-order polynomial provided the best fit. The initial plate velocity shown in the right-hand column of Table 1 represents this initial velocity.

## C. ANALYSIS

The first area of analysis was to establish the free-surface initial velocity of the top plate. It was observed that the top plate and concrete block moved off together and were projected upward essentially intact. This observation indicated that the entire impulse imparted to the concrete-steel plate structure was trapped. However, after motion began, there was a question as to whether the pressure pulse generated by the explosive charge continued to accelerate or have an effect on the concrete itself. A review of the displacement-time history of the various charges was instituted.

This review consisted primarily of computing a least-squares fit to the data. If the pressure pulse did not exist after the first motion, then the data should fit a second-order polynomial of the following form:

$$d = v_o t - \tfrac{1}{2} g t^2 \qquad (1)$$

TABLE 1. TEST SUMMARY

| Test Number | Charge Weight (gm) | Stand-Off Distance[1] (cm) | Cone Angle (deg) | Initial Velocity (cm/sec) |
|---|---|---|---|---|
| 1 | 500 | 15 | 90 | 1204 |
| 1R | 125 | 15 | 90 | 551 |
| 2 | 500 | 30 | 60 | 676 |
| 2R | 250 | 30 | 60 | 434 |
| 3 | 500 | 15 | 60 | 988 |
| 3R | 250 | 15 | 60 | 650 |
| 4 | 500 | 60 | 60 | 462 |
| 4R | 250 | 60 | 60 | 193 |
| 5 | 500 | C | 60 | 1473 |
| 5R | 250 | C | 60 | 894 |
| 6 | 500 | 60 | 20 | 378 |
| 6R | 250 | 60 | 20 | 196 |
| 7 | 500 | 30 | 20 | 345 |
| 7R | 250 | 30 | 20 | 226 |
| 8 | 250 | 15 | 20 | 348 |
| 9 | 250 | C | 20 | 444 |
| 10 | 125 | 60 | 160 | 262 |
| 11 | 125 | 30 | 160 | 536 |
| 12 | 250 | 60 | 30 | 345 |
| 13 | 250 | 30 | 30 | 366 |
| 14 | 67.5 | 15 | 160 | 470 |
| 15 | 67.5 | C | 160 | 841 |
| 16 | 135 | 15 | 30 | 351 |
| 17 | 250 | C | 30 | 876 |
| 18 | 250 | 60 | 90 | 338 |
| 19 | 125 | 30 | 90 | 406 |
| 20 | 125 | C | 90 | 952 |
| 21 | 250 | 60 | 45 | 315 |

(1) C designates Contact Charge

TABLE 1. TEST SUMMARY (CONCLUDED)

| Test Number | Charge Weight (gm) | Stand-Off Distance[1] (cm) | Cone Angle (deg) | Initial Velocity (cm/sec) |
|---|---|---|---|---|
| 22 | 250 | 30 | 45 | 368 |
| 23 | 250 | 60 | 135 | 470 |
| 23R | 125 | 60 | 135 | 272 |
| 24 | 125 | 30 | 135 | 472 |
| 25 | 250 | 15 | 45 | 612 |
| 26 | 250 | C | 45 | 932 |
| 27 | 125 | C | 135 | 709 |
| 28 | 125 | 15 | 135 | 399 |

where $d$ = displacement (cm)

$v_o$ = initial velocity (cm/sec)

$g$ = gravitation constant (980 cm/sec$^2$)

$t$ = time (seconds)

However, if there is continued pulse, it would be expected to be of the exponential decreasing type of force. The total force could then be represented by the equation:

$$F = -mg + A\, e^{-t/t_o} \qquad (2)$$

$F$ = force (dynes)

$m$ = total structure mass (gms)

$A, t_o$ = constants (to be determined)

This function can be expanded to a third-order polynomial where the two unknowns (A and $t_o$) can be determined from a third-order least-squares fit to the data.

Comparing the results of the second- and third-order least-squares fit showed that the time constant, $t_o$, was consistently negative. For this to be true, the pressure pulse must be increasing as it expands. This event was deemed physically unacceptable; therefore, the second-order curve data was accepted as being evidence that the initial velocity was the result of an impulse function and that the concrete cone-steel structure acted as a free-flight object after being impulsed. Thus, the initial velocity of the structure could be determined from a second-order least-squares fit. The results of this analysis are given in Table 2 and Figure 6.

Having established the initial velocity for the various tests, the data were plotted to ascertain the effect of cone angle. Initial velocity is plotted in Figure 6 as a function of cone angle. The 250-grain charge is used as a baseline. Where data points or multiple data points are available, the initial velocity for other charge weights have been scaled by

TABLE 2. INITIAL VELOCITY DATA

| Stand-Off Distance (cm) | Charge Weight (grams) | Initial Velocity* (cm/sec) Cone Angle (degrees) | | | | | | |
|---|---|---|---|---|---|---|---|---|
| | | 20 | 30 | 45 | 60 | 90 | 135 | 160 |
| Contact | 67.5 | | | | | | | 841 |
| | 125 | | | | | 952 | 709 | |
| | 250 | 444 | 876 | 932 | 894 | | | |
| | 500 | | | | 1473 | | | |
| 15 | 67.5 | | | | | | | 470 |
| | 125 | | 351 | | | 551 | 399 | |
| | 250 | 348 | | 612 | 650 | | | |
| | 500 | | | | 988 | 1204 | | |
| 30 | 67.5 | | | | | | | |
| | 125 | | | | | 406 | 472 | 536 |
| | 250 | 226 | 366 | 368 | 434 | | | |
| | 500 | 345 | | | 676 | | | |
| 60 | 67.5 | | | | | | | |
| | 125 | | | | | | 272 | 262 |
| | 250 | 196 | 345 | 315 | 193 | 338 | 470 | |
| | 500 | 378 | | | 462 | | | |

*Scaled velocity data normalized to 250 gram charge

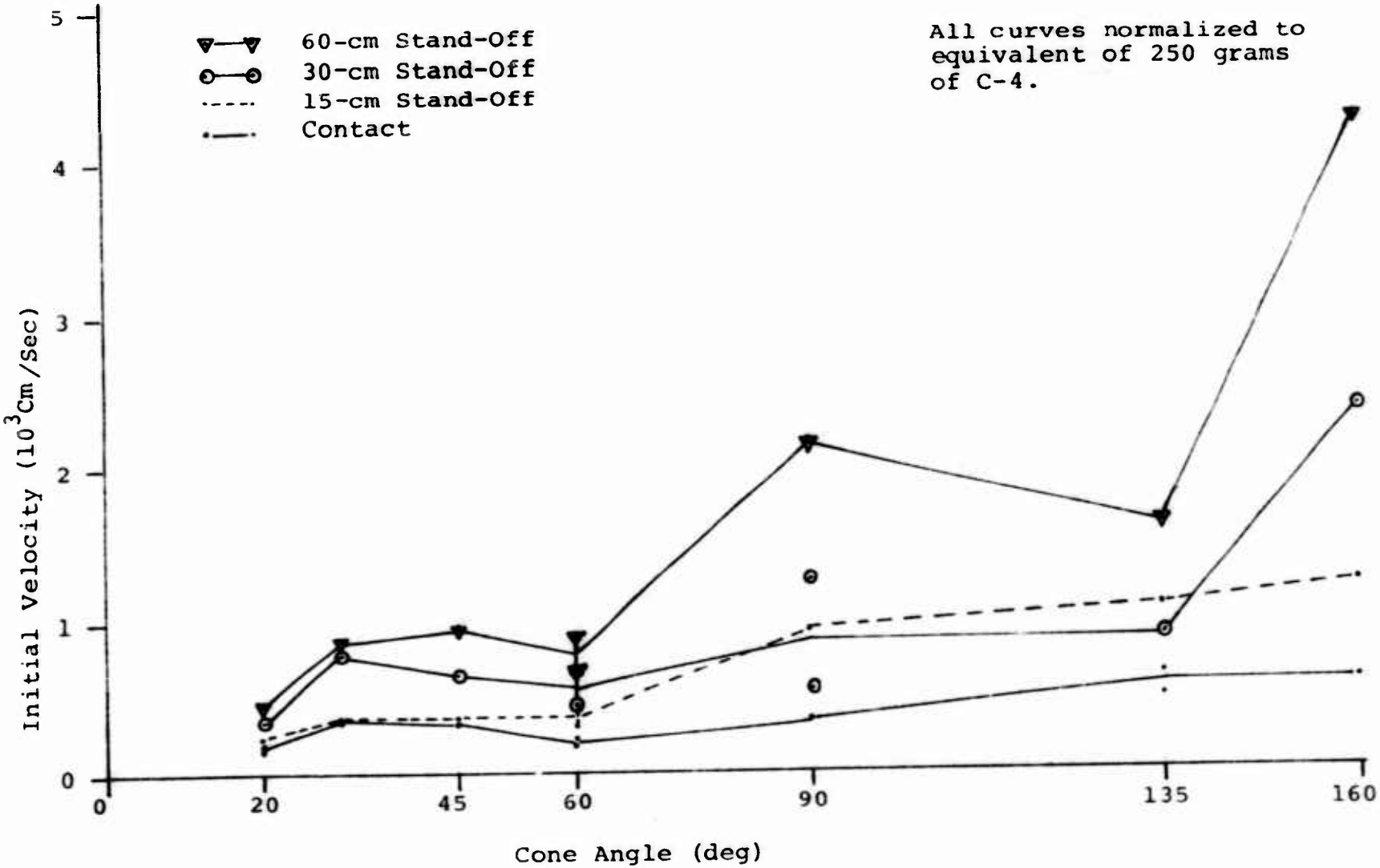


Figure 6. Initial Velocity Versus Cone Angle

a factor of 2.245 (i.e., 2 raised to the 7/6th power). This scaling factor is for scaling of impulse as a function of charge weight. For clarity's sake, the points were connected by straight lines to show the general trend of the data.

The data show that there is a dip at 60 degrees for all stand-offs in a monotonically increasing function of cone angle and one at 135 degrees for the shorter stand-off distances. One would expect a monotonically increasing function with cone angle. The impulse at larger stand-off distances may be expected to vary inversely as a function of the radius raised to the 5/2 power (Reference 1). A closed form solution is not possible for the test geometry. Using an inverse square and cube function (see Appendix B), a monotonically increasing impulse with cone angle is predicted. For the constant mass systems used during the tests, a monotonically increasing velocity should exist as the cone angle increases.

## D. CONCLUSIONS

Based on the free-surface tests, the initial velocity data indicates that there are effects of coupling between the soil and the concrete at the shallow cone angles, i.e., 20, 30, 45 degrees, which would tend to increase the force being applied to the concrete surface a a level above that predicted by an inverse square or inverse cube type of loading function. Further, both the contact and 15-centimeter stand-off configuration show reduced initial velocities for the 135-degree cone tests.

These results lead to the conclusion that hydrostatic-type loading and simple geometrical considerations do not adequately predict the actual response. Further investigations were indicated and planned to verify these findings using different experimental techniques.

## SECTION III

## CONSTRAINED CONFIGURATION TESTS

Conclusions drawn from the free-surface tests, described in the preceding section, indicated that the impulse impinging on the concrete structure shows reduced values when 60- and 135-degree cones are used. The reduced values at 60-degree cones are consistent at all stand-off distances, while the 135-degree cones had reduced velocities at contact and 15-centimeter stand-off. A reduced velocity at 30-centimeter stand-off may also exist. In order to verify these phenomena, seven additional tests were conducted where the top surface was constrained from free motion. The force of constrainment was measured as a function of time so both peak force and positive phase impulse could be determined. A stand-off of 30 centimeters was used since the free-surface tests showed this regime to be a possible transition distance.

To check the transmitted impulse magnitude by electronic means, a constrained test set-up was developed. Quartz pressure gages were used to measure the force applied to the steel flyer plate by a buried explosive charge. The total impulse (psi ms) was then measured from Polaroid® picures taken of the oscilloscope trace. This method gave a quantitative impulse and peak force transmission as a function of cone angle. Stand-off distance and charge size were held constant at 30 centimeters and 250 grams of C-4, respectively.

### A. TEST GEOMETRY AND SET-UP

The basic test geometry is the same as used in the free-surface tests except that massive confinement was used to constrain the steel disks. Figure 7 shows the method used to confine the steel disks/pressure gage assembly.

The explosive charge (250 grams of C-4) was buried beneath the cone at a stand-off of 30 centimeters. The charge was placed on the longitudinal axis of the cone assembly. Soil was packed around the cone until the cone/cylinder junction was flush with the free-soil surface. A steel disk, 2 inches thick, was then attached to the top of the cone. A Kistler type 907A quartz force gage was placed on the longitudinal axis; then a cover plate 2 inches thick was placed on top of the gage.

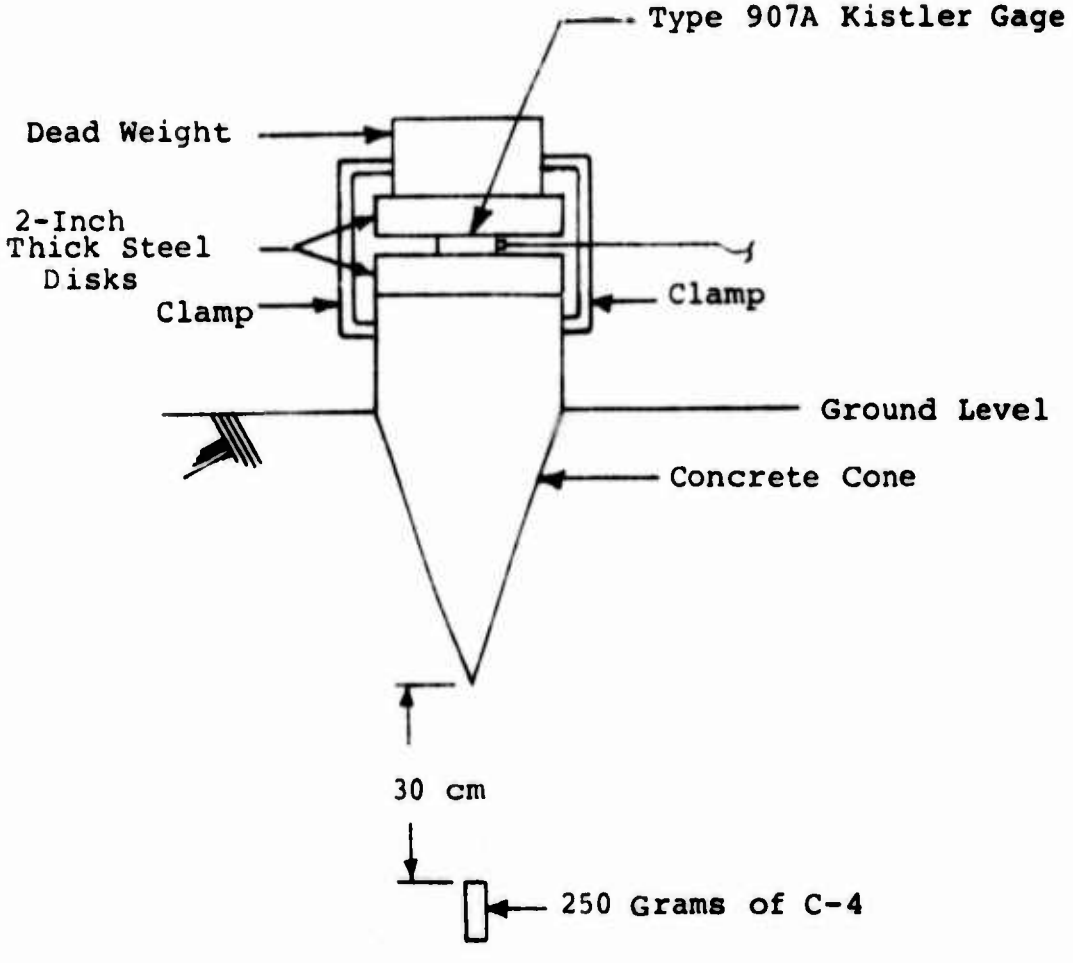


Figure 7. Constrained Configuration Test Set Up

This sandwich of gage, concrete cone, and steel disks was then clamped rigidly together. A dead weight of 227 pounds evenly distributed was then attached to the top steel disk. Including the upper steel disk, clamps, and dead weight, the gage was restrained by 310 pounds for every test. The total weight of each cone assembly as a function of cone angle is listed in Table 3.

TABLE 3. WEIGHT OF CONE ASSEMBLY

| Cone Angle (degrees) | Total Weight (pounds) |
|---|---|
| 20 | 435 |
| 30 | 506 |
| 45 | 434 |
| 60 | 447 |
| 90 | 448 |
| 135 | 445 |
| 160 | 445 |

1. Instrumentation

For the constrained test series, a piezoelectric type pressure gage was used to measure the force imparted to the top steel disk. This type gage consists of a quartz crystal cut in the shape of a donut with cover plates on each side. Compressing or stressing the crystal normal to its flat surface causes a charge (in picocoulombs) to be generated. This charge was modified by a high-impedance charge amplifier to a proportional voltage. This voltage was then used as an oscilloscope input. Figure 8 is a diagram of the test instrumentation while Figure 9 is a photograph of gages and charge amplifiers.

Figure 9. Kistler Gage and Amplifier

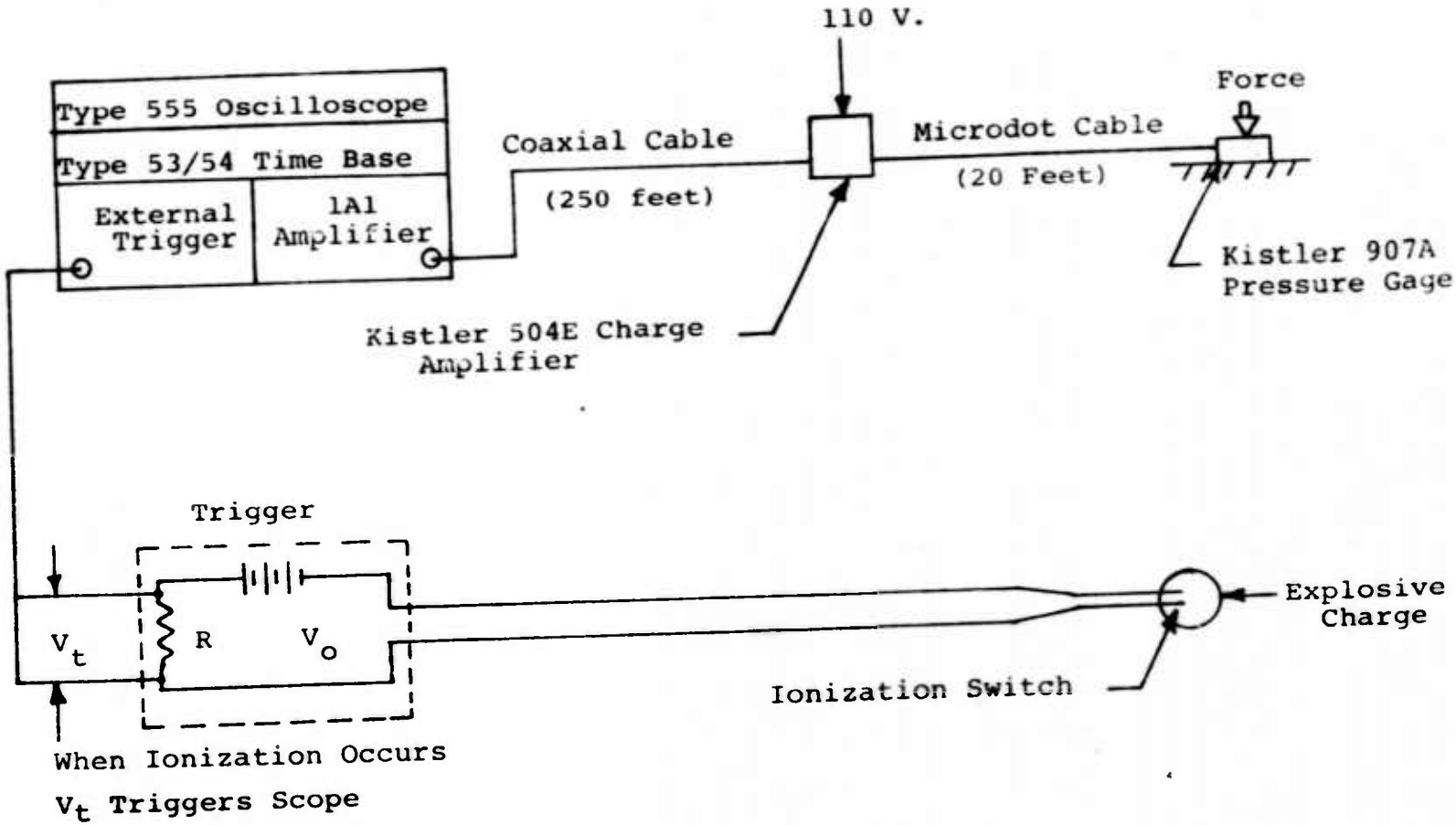


Figure 8. Electronics System - Constrained Tests

The quartz gage was a Kistler type 907A ring gage. This gage has a nominal load capability of 90,000 pounds force. The charge obtained from the gage was fed through low capacitance cable (Microdot) to a type 504E charge amplifier (Kistler).

The function of this amplifier was to convert the high impedance charge signal into a proportional low level voltage which could be displayed on an oscilloscope screen. Conversion of charge (picocoulombs) into voltage also allowed use of a long length of regular coaxial cable (type RG58 C/U) with minimal signal degradation.

The low level signal was fed into a Tektronics type 555 dual trace oscilloscope. Type 1A1 preamplifiers were used to amplify the signal, while a type 53/54 time base unit supplied the horizontal sweep.

The trace was photographed by a Poloroid ® type C-12 oscilloscope camera. Because of the large physical distance (250 feet) between the test set-up and instrumentation bunker, it was necessary to remotely trigger the scope at the instant of detonation. A normally open trigger wire was embedded in the explosive. The ionized products of combustion completed the circuit and triggered the sweep. The camera, which had its diaphragm opened just prior to detonation, then recorded the pressure pulse. This method of using an ionization switch to trigger the sweep has been found to be an extremely reliable and safe method of synchronizing widely separated events. The firing circuit used for these tests was the same one used for the free-surface tests.

B. FREE-SOIL DATA

Prior to running full-scale tests using Kistler gages, some reduced-scale tests were conducted to determine what force magnitudes would be encountered. The test set-up shown in Figure 10 was chosen to simulate the free-soil pressures encountered by the cone/disk assembly.

The soil was carefully packed around the gage, especially along its front surface, to insure good force transmission. Table 4 gives the results of these tests.

These tests used fully calibrated gages and the long (250 feet) signal cables used for the restrained tests. Figure 11 is a typical trace obtained from these tests. Measuring the

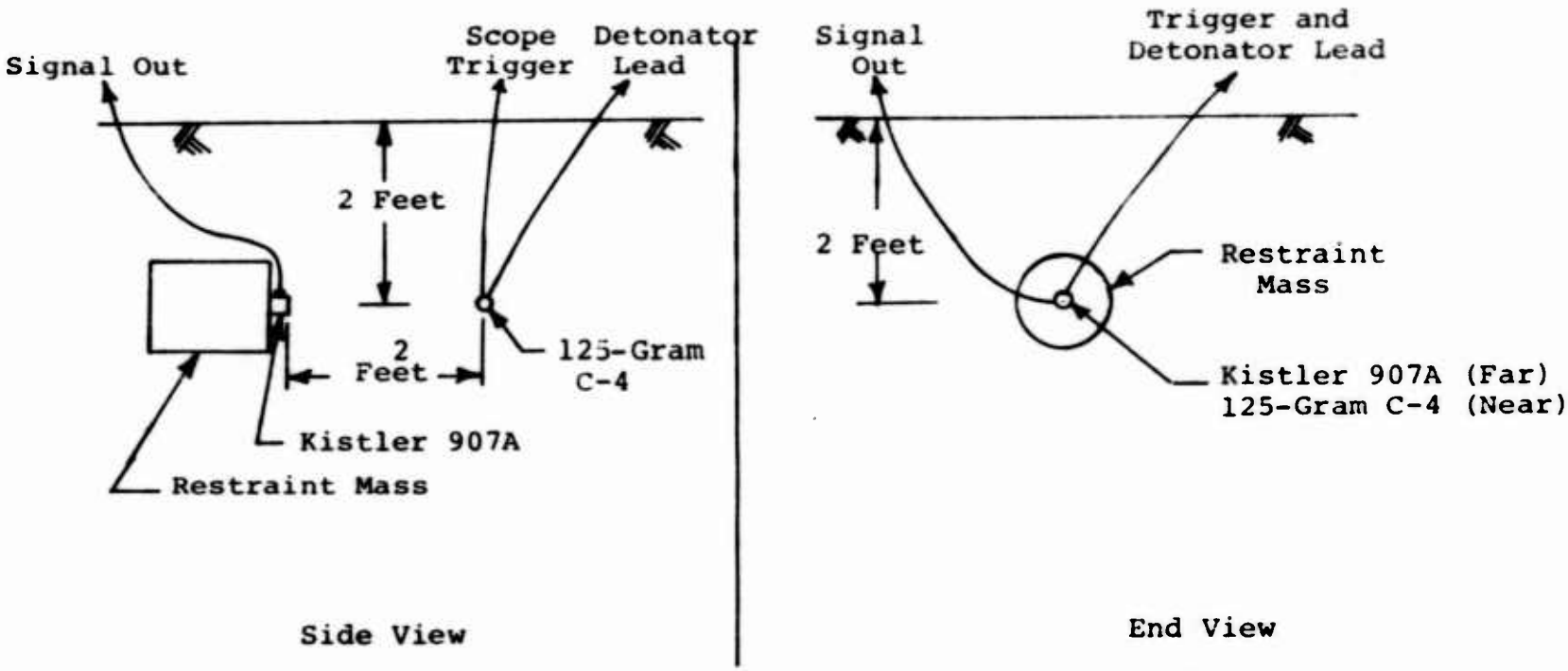


Figure 10. Free Soil Calibration Test Set-Up

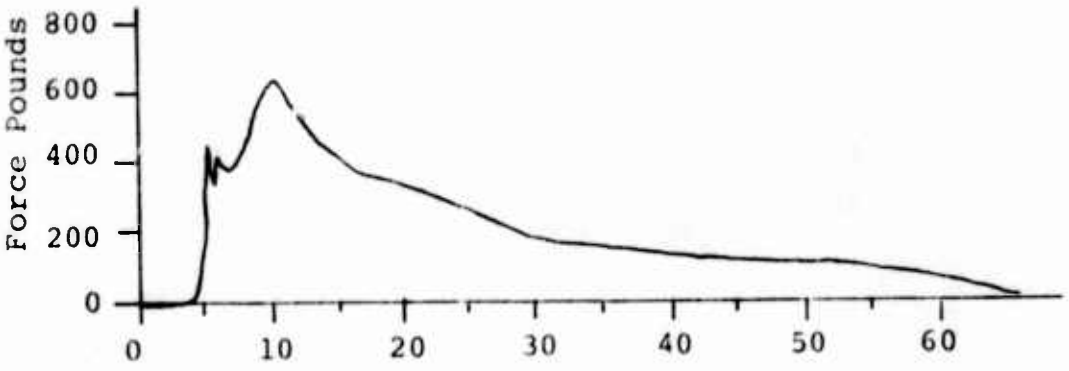


Time: ms

Dry Soil

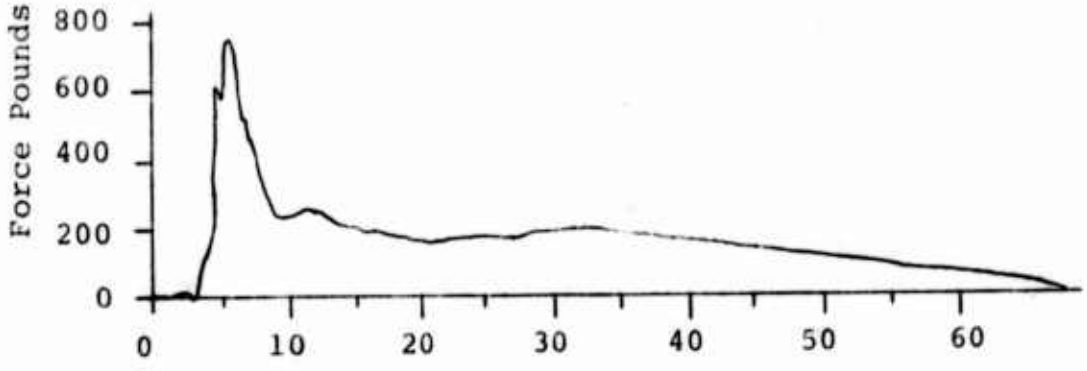


Time: ms

Damp Soil

Figure 11. Free-Soil Force Profiles

TABLE 4. FREE SOIL CALIBRATION TESTS

| Test | Peak Force (lb) | Total Impulse (lb msec) |
|---|---|---|
| 1 | 502 | 6,968 |
| 2 | 643 | 17,420 |
| 3 | 548 | 13,190 |
| 4 | 750 | no data |
| 5 | 750 | 14,149 |

the average delay from sweep trigger to pressure pulse rise gives a time delay of 3.84 milliseconds which, with a stand-off of 2 feet, gives a free-soil velocity of 521 feet/second. This velocity was the same with dry or damp soil. The total impulse was similar whether the soil was dry or damp, but the peak force was greater with wet soil.

C. TEST RESULTS

Using the peak levels, the maximum force generated on the gage was determined. Figure 12 is a plot of the maximum force as a function of cone angle. The free-surface test velocities for 20-, 30- and 45-degree cones exceed the velocity obtained with a 60-degree cone. In these tests, the maximum force generated with 20-, 30- and 45-degree cones exceeded the 60-degree cone value. The general trend observed in the free-surface tests exists here; namely, the load level appears to maintain itself at the smaller cone angles, i.e., below 60 degrees.

While the peak force cannot be correlated to the free-surface velocity, the impulse can. In the free-surface tests a second order polynomial was fit to the displacement-time data since all impulse appeared to be trapped prior to initial motion. Figure 13 is a plot of impulse as a function of cone angle, and Table 5 contains force and impulse data from these constrained tests.

Two deviations from a monotonically increasing function are noted. One exists at 60 degrees and the other at 135 degrees.

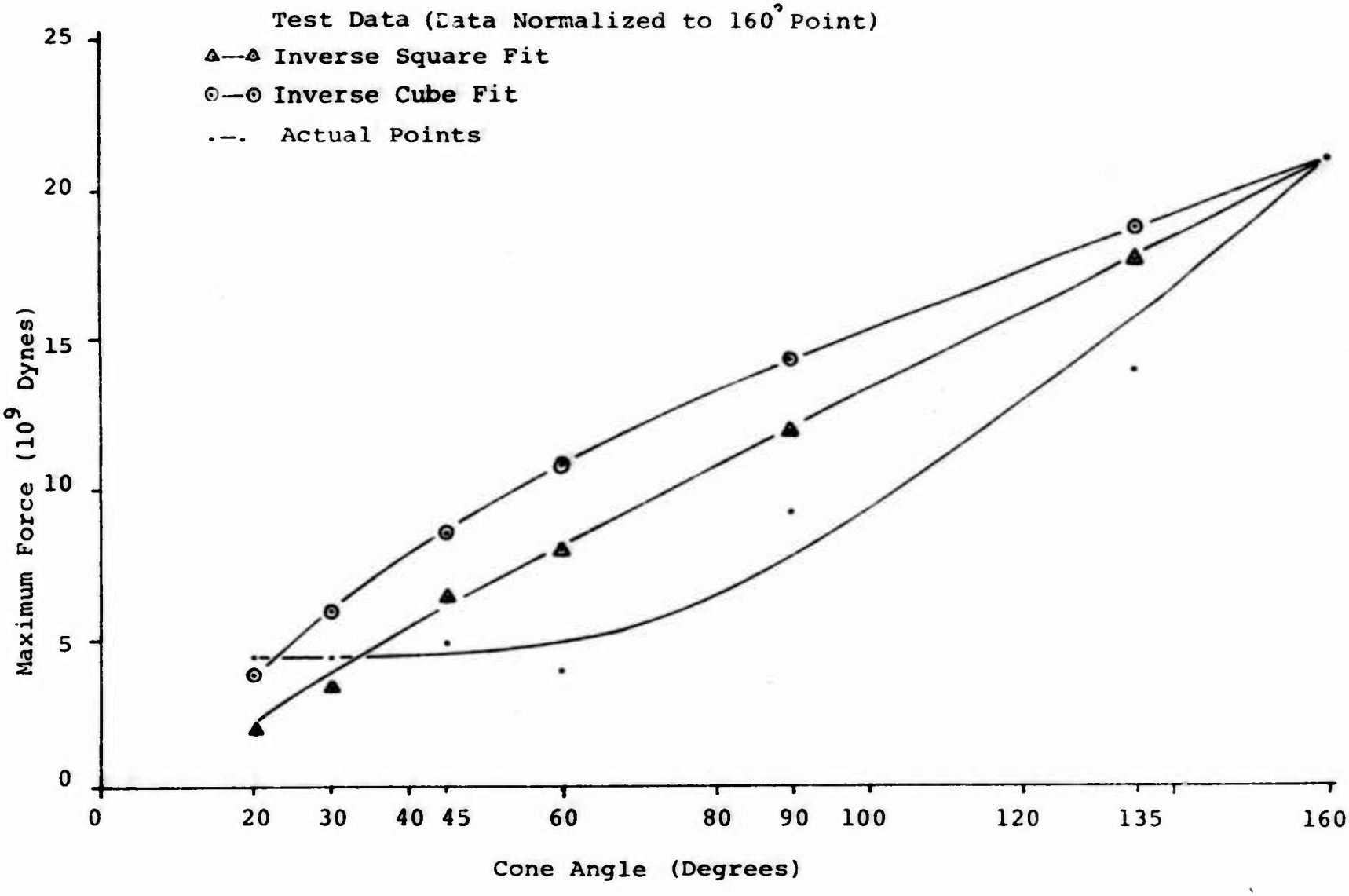


Figure 12. Maximum Force Versus Cone Angle

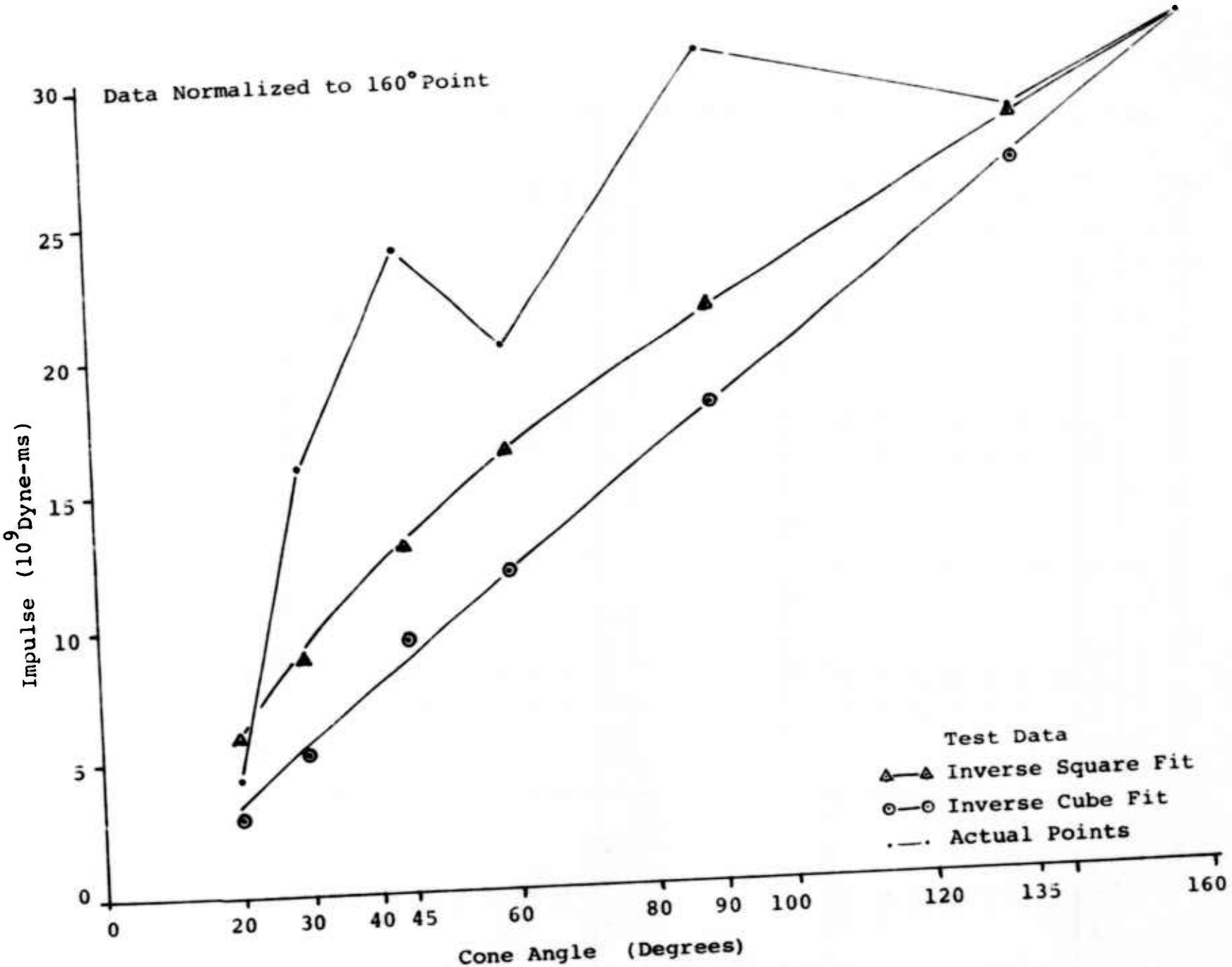


Figure 13. Total Impulse Versus Cone Angle

TABLE 5. FORCE AND IMPULSE AS FUNCTION OF CONE ANGLE

| Cone Angle (degrees) | Maximum Force ($10^9$ dynes) | Inverse Square (fit) | Inverse Cube (fit) |
|---|---|---|---|
| 20 | 4.45 | 3.88 | 1.93 |
| 30 | 4.45 | 5.90 | 3.38 |
| 45 | 4.94 | 8.50 | 6.29 |
| 60 | 3.95 | 10.67 | 7.81 |
| 90 | 9.11 | 14.20 | 11.76 |
| 135 | 13.96 | 18.60 | 17.50 |
| 160 | 21.00 | 21.00 | 21.00 |

Maximum Force Versus Cone Angle

| Cone Angle (degrees) | Maximum Force ($10^9$ dyne-ms) | Inverse Square (fit) | Inverse Cube (fit) |
|---|---|---|---|
| 20 | 4.25 | 5.84 | 2.90 |
| 30 | 15.35 | 8.88 | 5.09 |
| 45 | 23.91 | 12.81 | 9.47 |
| 60 | 20.27 | 16.07 | 11.76 |
| 90 | 30.88 | 21.38 | 17.71 |
| 135 | 28.88 | 28.00 | 26.35 |
| 160 | 31.62 | 31.62 | 31.62 |

Impulse Versus Cone Angle

In light of the top constraint allowing for some motion of the steel plate, the indicated impulse is less than the total impulse. The total impulse contributed to upward motion of the concrete cone-steel plate configuration as well as to the constraint mass.

Normalizing the inverse square and inverse cube functions given in Appendix B to the 160-degree cone data, the peak force function depicted in Figure 12 generally lies beneath both the inverse square and the inverse cube plots. Further, the force function is generally a concave function while the inverse square and inverse cube are convex. Conversely, in the impulse data the impulse function is generally converse as is the inverse square and inverse cube data with the impulse lying above the theoretical curves.

## D. CONCLUSIONS

The results of the seven constrained configuration tests are consistent with the 36 free-surface tests. There appears to be sustained and higher pressure levels observed when a relatively shallow angle of incidence exists. The peak forces do not drop off at a rate predicted by either an inverse square or inverse cube type of pressure decrease with radius. Rather, they level off at the shallow levels. Contrary to this, one notes that the impulse does drop off at shallow angles with definite anomalies at the 60- and 135-degree points.

## SECTION IV

## CONCLUSIONS AND RECOMMENDATIONS

The following conclusions and recommendations are based on the 36 tests that were conducted to measure the free-surface velocity of a concrete-steel mass dynamically loaded by explosive charges and on the 7 tests using the same configuration except constraining the upper surface.

### A. CONCLUSIONS

Based on the free-surface tests, the initial velocity data indicates that there are effects of coupling between the soil and the concrete at the shallow angles. These effects tend to increase the force being applied to the concrete surface at a level of pressure above the inverse square or inverse cube type of loading. Further, both contact and 15-centimeter stand-off configurations show reduced initial velocities for the 135-degree cone test. This result leads to the conclusion that hydrostatic-type loading and simple geometrical considerations do not adequately predict the actual response.

Further, for the close field work that is being done in these tests, the variation of impulse has been assumed to be a function of charge weight raised to the 7/6 power. This is the scaling factor used for impulse at the longer stand-off distances. While one would expect experimental variation in the data points, the predicted variations between the various charge weights indicate this simple type of scaling may be inadequate in the near field.

Using a single charge weight and using constraints, seven tests were conducted to measure the maximum force generated by a charge against a cone. The peak force data were consistent with those obtained in the free-surface tests. Mainly, the forces do not drop off at a rate predicted by the inverse square or inverse cube type of pressure decrease with radius. Rather, the force levels off at the shallow angle.

Contrary to this, one notes that the impulse does drop off at the shallow angle with definite anomalies occurring at the 60- and 135-degree cone data points.

The conclusion drawn from these tests is that oblique earth shock wave impingment on a concrete structure results in greater force levels (pressure levels) being generated on the concrete structure than would be expected from the use of a hydrostatic type of loading function and wave front impingement angles.

## B. RECOMMENDATIONS

Based on the results of the initial studies, it is recommended that a two-phase program be established to further define the soil concrete interface mechanics. The two phases should be theoretical and experimental programs. The theoretical stage should be concerned with applying continued mechanics computer codes to establish the shock front phenomena. The shock characteristics of the soil and interaction with concrete as the waves travel along the cone, with adequate allowances being made for venting once the shock wave reaches the free surface of the soil, should be modeled.

The second area should consist of experimental programs to continue testing using the constrained configuration where a rigid constraint is used to limit the top surface motion of the plate. This experimental series would give the total impulse imparted to the concrete cone-steel plate structure. With use of various size charges, the effect of charge weight can be better defined.

Thus, through the use of mathematical simulation and experimental data, the mechanics of a shock concrete interface can better be understood and applied to analysis of underground concrete structures.



(The reverse of this page is blank.)

## APPENDIX A

## TIME-DISPLACEMENT DATA

The following pages list the time-displacement data as taken from high-speed camera film. The first column measures the vertical displacement from the top plate. A 2-inch (5.08 centimeter) increment was used for the displacement in general. There are those areas where readings could not be made because of smoke obscuration or other difficulties along that line, such as maximum height plate.

Listed under each of the test numbers is the time, in seconds for the plate to reach the given height. On tests 4-R, 6-R, 7-R, and 10, the top measurement was not an even number of inches and an actual data point was measured at an odd number of inches. The exact number is in parentheses at the time data point and should be used, as opposed to the inch-displacement on the left column.

Using this data and a second-order least-squares fit, the initial velocity for this data is given at the bottom of the tables in both inches per second and centimeters per second.

TABLE A-1. DISPLACEMENT-TIME DATA

| Vertical Displacement (inches) | Time (seconds) Test Number | | | | | |
|---|---|---|---|---|---|---|
| | 1 | 1R | 2 | 2R | 3 | 3R |
| 0 | 0.00000 | 0.00000 | 0.00000 | 0.00000 | 0.00000 | 0.00000 |
| 2 | 0.00422 | 0.01249 | 0.01066 | 0.02092 | 0.00638 | 0.00813 |
| 4 | 0.00802 | 0.02196 | 0.01645 | 0.03479 | 0.01148 | 0.01342 |
| 6 | 0.01223 | 0.03283 | 0.02612 | 0.04511 | 0.01913 | 0.02201 |
| 8 | 0.01545 | 0.04385 | 0.09223 | 0.05656 | 0.02359 | 0.02944 |
| 10 | 0.02007 | 0.07729 | | 0.07031 | 0.02853 | 0.03652 |
| 12 | 0.02454 | 0.06305 | | 0.08157 | 0.03283 | 0.04405 |
| 14 | 0.02872 | 0.07277 | | 0.09433 | 0.03903 | 0.05111 |
| 16 | 0.03289 | 0.08263 | 0.10374 | 0.10754 | 0.04380 | 0.05984 |
| 18 | 0.3953 | | | 0.12155 | 0.04935 | 0.05861 |
| 20 | 0.04809 | 0.09186 | | 0.13615 | 0.05411 | 0.06549 |
| 22 | 0 06600 | | | 0.15387 | | 0.07367 |
| 24 | | 0.11202 | | 0.17108 | 0.06440 | 0.08151 |
| 26 | | 0.13591 | | 0.19219 | | 0.08951 |
| 28 | | | | 0.21276 | 0.07467 | 0.09668 |
| 30 | | | | 0.22885 | | 0.10545 |
| 32 | | | | 0.26665 | | 0.11518 |
| Initial Velocity (inches/sec) | 474 | 217 | 266 | 171 | 389 | 256 |
| (cm/sec) | 1204 | 551 | 676 | 434 | 988 | 650 |

TABLE A-1. DISPLACEMENT-TIME DATA (CONTINUED)

| Vertical Displacement (inches) | Time (seconds) Test Number 4 | 4R | 5 | 5R | 6 | 6R |
|---|---|---|---|---|---|---|
| 0 | 0.00000 | 0.00000 | 0.00000 | 0.00000 | 0.00000 | 0.00000 |
| 2 | 0.01469 | 0.02633 | 0.00341 | 0.00455 | 0.01555 | 0.02593 |
| 4 | 0.02737 | 0.05655 | 0.00681 | 0.00796 | 0.03303 | 0.06029 |
| 6 | 0.03710 | 0.08438 | 0.00981 | 0.01428 | 0.04597 | 0.11174 |
| 8 | 0.05019 | 0.11586 | 0.01281 | 0.01865 | 0.05956 | 0.19651 (7) |
| 10 | 0.06140 | 0.16353 | 0.01561 | 0.02431 | 0.08514 | |
| 12 | 0.07228 | 0.22374 (11) | 0.01820 | 0.02932 | 0.10161 | |
| 14 | 0.08268 | | 0.02609 | 0.03465 | 0.11477 | |
| 16 | 0.09152 | | 0.02907 | 0.03982 | 0.12934 | |
| 18 | 0.11040 | | 0.03225 | 0.04643 | 0.15510 | |
| 20 | 0.12865 | | 0.03542 | 0.05126 | 0.16893 | |
| 22 | 0.14247 | | 0.03879 | 0.05720 | 0.19231 | |
| 24 | 0.15051 | | 0.04117 | 0.06218 | 0.22835 | |
| 26 | 0.16669 | | 0.04506 | 0.06844 | | |
| 28 | 0.19383 | | 0.04912 | 0.07454 | | |
| 30 | | | | 0.08047 | | |
| 32 | | | | 0.08671 | | |
| Initial Velocity (inches/sec) | 182 | 76 | 580 | 352 | 149 | 77 |
| (cm/sec) | 464 | 193 | 1473 | 894 | 378 | 196 |

TABLE A-1. DISPLACEMENT-TIME DATA (CONTINUED)

| Vertical Displacement (inches) | Time (seconds) Test Number 7 | 7R | 8 | 9 | 10 | 11 |
|---|---|---|---|---|---|---|
| 0 | 0.00000 | 0.00000 | 0.00000 | 0.00000 | 0.00000 | 0.00000 |
| 2 | 0.01322 | 0.02234 | 0.01459 | 0.01144 | 0.01023 | 0.01141 |
| 4 | 0.02961 | 0.04824 | 0.02933 | 0.02319 | 0.03402 | 0.01912 |
| 6 | 0.04852 | 0.07291 | 0.04508 | 0.03694 | 0.04988 | 0.03231 |
| 8 | 0.06680 | 0.10873 | 0.06037 | 0.05027 | 0.07475 | 0.04307 |
| 10 | 0.08836 | 0.15264 | 0.07762 | 0.06610 | 0.10169 | 0.05240 |
| 12 | 0.09954 | 0.22101 | 0.09282 | 0.08222 | 0.13812 | 0.16163 |
| 14 | 0.12364 | 0.27373 (13) | 0.11027 | 0.10242 | 0.16772 | 0.07098 |
| 16 | 0.14452 | | 0.12586 | 0.12307 | 0.25080 (15) | 0.08031 |
| 18 | 0.26618 | | 0.13828 | 0.14180 | | 0.09118 |
| 20 | 0.29367 | | 0.16446 | 0.16474 | | 0.10359 |
| 22 | 0.33401 | | 0.31379 | | | 0.11950 |
| 24 | 0.36645 | | | 0.20701 | | 0.12883 |
| 26 | | | | | | |
| 28 | | | | 0.29206 | | |
| 30 | | | | | | |
| 32 | | | | | | |
| Initial Velocity (inches/sec) | 136 | 89 | 137 | 175 | 103 | 211 |
| (cm/sec) | 345 | 226 | 348 | 444 | 262 | 536 |

TABLE A-1. DISPLACEMENT-TIME DATA (CONTINUED)

| Vertical Displacement (inches) | Time (seconds) Test Number | | | | | |
|---|---|---|---|---|---|---|
| | 12 | 13 | 14 | 15 | 16 | 17 |
| 0 | 0.00000 | 0.00000 | 0.00000 | 0.00000 | 0.00000 | 0.00000 |
| 2 | 0.01449 | 0.01770 | 0.01035 | 0.00619 | 0.01512 | 0.00721 |
| 4 | 0.02816 | 0.03159 | 0.02228 | 0.01206 | 0.02837 | 0.01459 |
| 6 | 0.04749 | 0.04690 | 0.02989 | 0.01885 | 0.04143 | 0.02095 |
| 8 | 0.06541 | 0.06492 | 0.04210 | 0.02441 | 0.05816 | 0.02769 |
| 10 | 0.09118 | 0.08628 | 0.05382 | 0.03243 | 0.02682 | 0.03233 |
| 12 | 0.10189 | 0.09580 | 0.06505 | 0.03783 | 0.10183 | 0.03777 |
| 14 | 0.12049 | 0.11734 | 0.07501 | 0.04277 | 0.11863 | 0.04527 |
| 16 | 0.14627 | 0.13559 | 0.08764 | 0.04972 | 0.13375 | 0.05000 |
| 18 | 0.16613 | 0.16393 | 0.09883 | 0.05604 | 0.15900 | 0.05559 |
| 20 | 0.20444 | 0.19815 | 0.11364 | 0.06205 | 0.18198 | 0.06160 |
| 22 | 0.24995 | 0.22496 | 0.12934 | 0.06866 | 0.24201 | 0.06749 |
| 24 | | 0.28566 | 0.14719 | 0.07510 | 0.27104 | 0.07219 |
| 26 | | | 0.16394 | 0.08291 | | 0.07785 |
| 28 | | | 0.17972 | 0.08934 | | 0.08525 |
| 30 | | | 0.20407 | 0.09592 | | |
| 32 | | | 0.22590 | | | |
| Initial Velocity | | | | | | |
| (inches/sec) | 136 | 144 | 185 | 331 | 138 | 345 |
| (cm/sec) | 345 | 366 | 470 | 841 | 351 | 876 |

TABLE A-1. DISPLACEMENT-TIME DATA (CONTINUED)

| Vertical Displacement (inches) | Time (seconds) Test Number | | | | | |
|---|---|---|---|---|---|---|
| | 18 | 19 | 20 | 21 | 22 | 23 |
| 0 | 0.00000 | 0.00000 | 0.00000 | 0.00000 | 0.00000 | 0.00000 |
| 2 | 0.01858 | 0.01190 | 0.00492 | 0.01474 | 0.01545 | 0.01521 |
| 4 | 0.03237 | 0.02807 | 0.01000 | 0.03228 | 0.02879 | 0.02845 |
| 6 | 0.04640 | 0.03911 | 0.01682 | 0.05130 | 0.04325 | 0.03871 |
| 8 | 0.06267 | 0.05439 | 0.02253 | 0.07550 | 0.05524 | 0.04940 |
| 10 | 0.08212 | 0.06445 | 0.02902 | 0.01013 | 0.07075 | 0.06130 |
| 12 | 0.10366 | 0.08281 | 0.03535 | 0.11927 | 0.08699 | 0.07350 |
| 14 | 0.12396 | 0.09768 | 0.04167 | 0.14816 | 0.10557 | 0.0[illegible]533 |
| 16 | 0.15062 | 0.11987 | 0.04799 | 0.17923 | 0.12851 | 0.09690 |
| 18 | 0.18156 | 0.13796 | 0.05446 | 0.22626 | 0.15562 | 0.10968 |
| 20 | 0.22320 | 0.15492 | 0.06013 | | 0.18963 | 0.12245 |
| 22 | 0.26913 | 0.17799 | 0.06690 | | 0.21866 | 0.13934 |
| 24 | | 0.19844 | 0.07413 | | 0.24618 | 0.15429 |
| 26 | | 0.22406 | 0.08151 | | | 0.17050 |
| 28 | | 0.25566 | 0.09568 | | | |
| 30 | | 0.28640 | | | | |
| 32 | | 0.34763 | | | | |
| Initial Velocity (inches/sec) | 133 | 160 | 375 | 124 | 145 | 185 |
| (cm/sec) | 338 | 406 | 952 | 315 | 368 | 470 |

TABLE A-1. DISPLACEMENT-TIME DATA (CONCLUDED)

| Vertical Displacement (inches) | Time (seconds) Test Number | | | | | |
|---|---|---|---|---|---|---|
| | 23R | 24 | 25 | 26 | 27 | 28 |
| 0 | 0.00000 | 0.00000 | 0.00000 | 0.00000 | 0.00000 | 0.00000 |
| 2 | 0.01831 | 0.01055 | 0.00770 | 0.00596 | 0.00585 | 0.00812 |
| 4 | 0.04037 | 0.02280 | 0.01669 | 0.01127 | 0.00970 | 0.01449 |
| 6 | 0.06096 | 0.03454 | 0.02598 | 0.01674 | 0.01447 | 0.02211 |
| 8 | 0.08212 | 0.04423 | 0.03509 | 0.02187 | 0.02039 | 0.02943 |
| 10 | 0.10587 | 0.05719 | 0.04240 | 0.02780 | 0.02682 | 0.03843 |
| 12 | 0.13481 | 0.06842 | 0.05229 | 0.03228 | 0.03234 | 0.12073 |
| 14 | 0.18393 | 0.08292 | 0.05957 | 0.03756 | 0.03739 | 0.13139 |
| 16 | 0.22478 | 0.09538 | 0.06975 | 0.04363 | 0.07869 | 0.13853 |
| 18 | 0.27124 (17) | 0.11048 | 0.07975 | 0.04874 | 0.08501 | 0.14809 |
| 20 | | 0.12540 | 0.18813 | 0.05496 | 0.19000 | 0.15370 |
| 22 | | 0.14167 | | 0.06102 | 0.09443 | 0.23850 |
| 24 | | 0.15374 | 0.10565 | 0.06580 | 0.10024 | 0.24758 |
| 26 | | 0.17107 | | 0.07216 | 0.10498 | 0.25605 |
| 28 | | 0.18638 | 0.12940 | 0.07803 | 0.11124 | 0.26574 |
| 30 | | 0.20462 | | 0.08548 | 0.11719 | |
| 32 | | | | | | |
| Initial Velocity | | | | | | |
| (inches/sec) | 107 | 186 | 241 | 367 | | 157 |
| (cm/sec) | 272 | 474 | 612 | 932 | 709 | 399 |

## APPENDIX B

## INVERSE SQUARE AND INVERSE CUBE FUNCTIONS

If it is assumed that the loading on the cone portion of the cone varies as the inverse square or inverse cube of the distance (r) from the charge center to the point of loading, then the vertical loading function (F) is given by:

$$F = \sin\theta \int_0^L p(r)\, A$$

where $L$ = length of cone

$\theta$ = one-half cone angle

$dA$ = differential area $p(r)$ is applied; and

$p(r) = k/r^2$ (inverse square)

$k/r^3$ (inverse cube)

The solution to the above integral is:

$$F = k\pi \sin^2\theta \; \{0.5 \ln(1+2\beta + \beta^2 \sec^2\theta) - \cot\theta\left[\tan^{-1}(1 + \beta\sec^2\theta)\cot\theta\right] + \cot\theta\left[\tan^{-1}\cot\theta\right]\} \text{ for inverse square}$$

where $\beta = L/d$

$d$ = stand-off distance, and

$F = -k\pi \left\{\left[(\beta+1)/\gamma^{1/2}\right] - 1/d\right\}$ (Inverse Cube)

where $\gamma = d^2 + 2dL + L^2 \sec^2\theta$

Figure B-1 plots $F/k\pi$ for the inverse square data and inverse cube data using a 30-centimeter stand-off distance.

| Cone Angle (degrees) | Inverse Square (F/kπ) | Inverse Cube (F/kπ) |
|---|---|---|
| 20 | 0.0585 | .00220 |
| 30 | .0890 | .00386 |
| 45 | .1283 | .00718 |
| 60 | .1610 | .00892 |
| 90 | .2142 | .01343 |
| 135 | .2806 | .01998 |
| 160 | .3168 | .02398 |

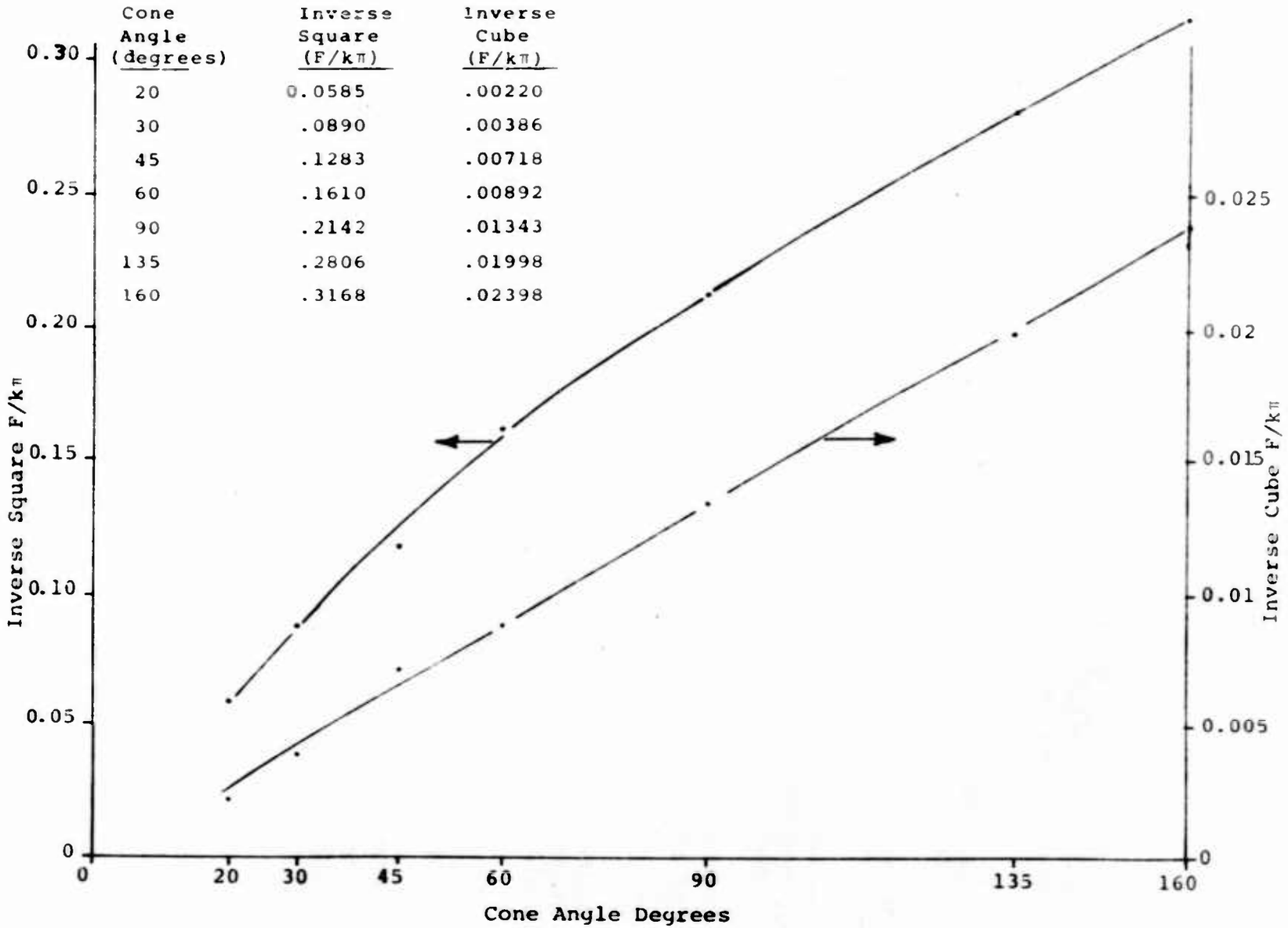


Figure B-1. Forcing Function Versus Cone Angle

## REFERENCES


1. NDRC Effects of Impact and Explosion, Volume 1, Office of Scientific Research and Development, National Defense Research Committee, Washington, D. C., 1946.

2. Levy, S. et. al. Full and Model Scale Tests of Baystructures. Technical Report 4168, Ammunition Engineering Dictorate Picatinny Arsenal, N. J., February 1971.

3. Fuehrer, H. Effects of Imbedded Munition, AFATL-TR-72-119 Air Force Armament Laboratory, Eglin AFB, FL, 1972.

4. Fuehrer, H. R. and Keeser, J. W., Vulnerability of Underground POL Storage Facilities, AFATL-TR-75-31, Air Force Armament Laboratory, Eglin AFB, FL, February 1975.

5. Fuehrer, J. R. and Keeser, J. W., Effects of Buffer Materials in Protection of Underground Structures. AFATL-TR-75-157, Air Force Armament Laboratory, Eglin AFB, FL, December 1975.

6. Godfrey, C. S., et. al., Calculation of Undergrcund and Surface Explosions, AFWL-TR-65-211, Air Force Weapons Laboratory, Kirtland AFB, N. M., June 1966.

7. AFM 88-22 Structures to Resist the Effects of Accidental Explosions, Department of the Army, Navy, and Air Force, June 1969.

8. Newmark, N. M. and Haltiwanger, J. D., Air Force Design Manual, Principles and Practice for Design of Hardened Structures. AFSWC-TDR-62-138, Air Force Special Weapons Center, Air Force Systems Command, Kirtland AFB, N. M., December 1962.

## INITIAL DISTRIBUTION

| | |
|---|---|
| HQ/USAF/RDQ | 1 |
| HQ USAF/SAMI | 1 |
| Defense Intelligence Agency/DB-4C3 | 1 |
| AUL (AUL/LSE-70-239) | 1 |
| HQ SAC/NRI | 1 |
| Nav Wpns Center/Code 3269 | 1 |
| Nav Wpns Center/Code 407 | 1 |
| AFSC Liaison Office/Code 143 | 2 |
| Ogden ALC/MMWM | 2 |
| AFATL/DLOSL | 9 |
| AFATL/DL | 1 |
| AFATL/DLJK | 1 |
| AFATL/DLJW | 1 |
| AFATL/DLD | 1 |
| AFATL/DLY | 1 |
| ADTC/XR | 1 |
| ADTC/SD | 2 |
| SACPO | 1 |
| USAFTAWC/OA | 1 |
| AFATL/DLYV | 4 |
| AFATL/DLYW | 1 |
| Southwest Research Institute | 1 |
| Orlando Technology, Inc. | 5 |
| Sundstrand Data Control, Inc. | 1 |
| Texas Tech University | 1 |
| Univ of Fla Grad Center | 1 |
| Univ of Florida | 1 |
| U.S. Army Engineer Waterways Experiment Station | 2 |
| AMXBR-VL | 1 |
| Defense Nuclear Agency/SPSS | 1 |
| Goodyear Aerospace Corp/Dept 456 | 1 |
| DDC | 2 |
| Oklahoma State University | 1 |
| Lockheed Missiles & Space Co., Inc. | 1 |
| ASD/ENFEA | 1 |
| TAWC/TRADOCLO | 1 |
| AFIS/INTA | 1 |



(The reverse of this page is blank)